Chiral phase transition within effective models with constituent quarks

O. Scavenius,[1] Á. Mócsy,[2] I. N. Mishustin,[1,3,4] and D. H. Rischke[4,5]
[1]*The Niels Bohr Institute, Blegdamsvej 17, DK-2100 Copenhagen Ø, Denmark*
[2]*School of Physics and Astronomy, University of Minnesota, Minneapolis, Minnesota 55455*
[3]*The Kurchatov Institute, Russian Research Center, Moscow RU-123182, Russia*
[4]*Institut für Theoretische Physik, J. W. Goethe Universität, D-60054 Frankfurt am Main, Germany*
[5]*RIKEN-BNL Research Center, Brookhaven National Laboratory, Upton, New York 11973*
(Received 19 July 2000; published 30 August 2001)

We study the chiral phase transition at nonzero temperature T and baryon chemical potential μ_B within the framework of the linear sigma model and the Nambu–Jona-Lasinio (NJL) model. For small bare quark masses we find in both models a smooth crossover transition for nonzero T and $\mu_B=0$ and a first order transition for $T=0$ and nonzero μ_B. We calculate explicitly the first order phase transition line and spinodal lines in the (T,μ_B) plane. As expected they all end at a critical point. We find that, in the linear sigma model, the sigma mass goes to zero at the critical point. This is in contrast to the NJL model, where the sigma mass, as defined in the random phase approximation, does not vanish. We also compute the adiabatic lines in the (T,μ_B) plane. Within the models studied here, the critical point does not serve as a ''focusing'' point in the adiabatic expansion.

DOI: 10.1103/PhysRevC.64.045202 PACS number(s): 11.30.Rd, 12.38.Mh, 12.38.Aw, 11.30.Qc

I. INTRODUCTION

Chiral symmetry is spontaneously broken in the QCD vacuum. Lattice QCD simulations at nonzero temperature T and zero baryon chemical potential μ_B indicate that chiral symmetry is restored above a temperature $T\sim 150$ MeV [1]. Even higher temperatures are believed to be created in nuclear collisions at ultrarelativistic energies. Consequently, a phase where chiral symmetry is transiently restored may be formed in these collisions. The subsequent expansion cools the system and takes it to the final hadronic state, where chiral symmetry is again spontaneously broken.

It is important to determine the order of the chiral transition, as this influences the dynamical evolution of the system. For instance, a first order transition may lead to a deflagration wave and to a ''stall'' in the expansion of the system [2]. It has been shown that a first order transition in rapidly expanding matter may manifest itself by strong nonstatistical fluctuations due to droplet formation [3]. In the case of strong supercooling it may lead to large fluctuations due to spinodal decomposition [4,5]. In a second order phase transition one may expect the appearance of critical fluctuations due to a large correlation length [6]. Experimentally, large-acceptance detectors are now able to measure average as well as event-by-event observables, which in principle allow one to distinguish between scenarios with a first order, a second order, or merely a crossover type of phase transition.

Theoretically, the QCD phase diagram in the (T,μ_B) plane has recently received much attention (see [6,8–10]). QCD with $N_f=2$ flavors of massless quarks has a global $SU(2)_L\times SU(2)_R$ symmetry. This symmetry is spontaneously broken in the QCD vacuum, such that the order parameter $\phi^{ij}\sim\langle\overline{q_L^i}q_R^j\rangle$ acquires a nonvanishing expectation value, where q^i is the quark field (i,j are the flavor indices). At zero baryon chemical potential, the effective theory for this order parameter is the same as the $O(4)$ model which has a second order phase transition. Therefore, by universality arguments [11], the chiral transition in $N_f=2$ QCD is likely to be of second order at $\mu_B=0$. Nonzero quark masses introduce a term in the QCD Lagrangian that explicitly breaks chiral symmetry. Then the second order transition becomes a crossover.

At nonzero baryon chemical potential, it is more difficult to infer the order of the chiral transition from universality arguments [12]. One commonly resorts to phenomenological models to describe the chiral transition in this case. Depending on the parameters of these models, they predict a first order, a second order, or a crossover transition. However, if there is a second order phase transition for $\mu_B=0$ and nonzero T and a first order transition for small T and nonzero μ_B, then there exists a tricritical point in the (T,μ_B) plane where the line of first order phase transitions meets the line of second order phase transitions. For nonzero quark masses, this tricritical point becomes a critical point.

It has recently been proposed [6] that this point could lead to interesting signatures in heavy-ion collisions at intermediate energies, if the evolution went through or close to this critical point. At this point, susceptibilities (e.g., the heat capacity) diverge, and the order parameter field becomes massless and consequently exhibits strong fluctuations, which could be detected in event-by-event observables.

In this paper we investigate the thermodynamics of two popular models of chiral dynamics, the linear sigma model coupled to quarks [13], and the Nambu–Jona-Lasinio (NJL) model [14]. Both models are tuned to reproduce correctly properties of the physical vacuum. Our goal is to study the chiral transition and to verify the existence of the critical point at nonzero chemical potential and temperature. We also study the behavior of isentropes in the vicinity of the phase transition line in the (T,μ_B) plane. These results can then be used in dynamical simulations to confront the predictions of Refs. [2–6] with experimental data.

The structure of the paper is as follows. In Sec. II we study the thermodynamics of the linear sigma model coupled to quarks. This part of the paper is an extension of our previous study in Ref. [16]. In Sec. III we do the same for the NJL model. Section IV presents numerical results. We conclude in Sec. V with a summary of our results. Our units are $\hbar=c=k_B=1$; the metric tensor is $g^{\mu\nu}=\mathrm{diag}(+,-,-,-)$.

II. THERMODYNAMICS OF THE LINEAR SIGMA MODEL

First we consider the linear sigma model which includes quark degrees of freedom. The model reads

$$\mathcal{L}=\bar{q}[i\gamma^\mu\partial_\mu-g(\sigma+i\gamma_5\vec{\tau}\cdot\vec{\pi})]q+\frac{1}{2}(\partial_\mu\sigma\partial^\mu\sigma+\partial_\mu\vec{\pi}\cdot\partial^\mu\vec{\pi})-U(\sigma,\vec{\pi}), \tag{1}$$

where the potential is

$$U(\sigma,\vec{\pi})=\frac{\lambda^2}{4}(\sigma^2+\vec{\pi}^2-v^2)^2-H\sigma. \tag{2}$$

Here q is the light quark field $q=(u,d)$. The scalar field σ and the pion field $\vec{\pi}=(\pi_1,\pi_2,\pi_3)$ together form a chiral field $\Phi=(\sigma,\vec{\pi})$. This Lagrangian is invariant under chiral $SU(2)_L\times SU(2)_R$ transformations if the explicit symmetry breaking term $H\sigma$ is zero. The parameters of the Lagrangian are usually chosen such that the chiral symmetry is spontaneously broken in the vacuum and the expectation values of the meson fields are $\langle\sigma\rangle=f_\pi$ and $\langle\vec{\pi}\rangle=0$, where $f_\pi=93$ MeV is the pion decay constant. The constant H is fixed by the partially conserved axial vector current (PCAC) relation which gives $H=f_\pi m_\pi^2$, where $m_\pi=138$ MeV is the pion mass. Then one finds $v^2=f_\pi^2-m_\pi^2/\lambda^2$. The coupling constant λ^2 is determined by the sigma mass $m_\sigma^2=2\lambda^2 f_\pi^2+m_\pi^2$, which we set to 600 MeV, yielding $\lambda^2\approx 20$. The coupling constant g is usually fixed by the requirement that the constituent quark mass in vacuum, $M_{\mathrm{vac}}=gf_\pi$, is about 1/3 of the nucleon mass, which gives $g\simeq 3.3$.

Let us consider a spatially uniform system in thermodynamical equilibrium at temperature T and quark chemical potential $\mu\equiv\mu_B/3$. In general, the grand partition function reads

$$\mathcal{Z}=\mathrm{Tr}\exp[-(\hat{\mathcal{H}}-\mu\hat{\mathcal{N}})/T]=\int\mathcal{D}\bar{q}\mathcal{D}q\mathcal{D}\sigma\mathcal{D}\vec{\pi}\exp\left[\int_x(\mathcal{L}+\mu\bar{q}\gamma^0 q)\right], \tag{3}$$

where $\int_x\equiv i\int_0^{1/T}dt\int_V d^3x$ and V is the volume of the system. Below we adopt the mean-field approximation, replacing σ and $\vec{\pi}$ in the exponent by their expectation values. In other words, we neglect both quantum and thermal fluctuations of the meson fields and retain only quarks and antiquarks as quantum fields. In this respect our model differs from other realizations of the sigma model, where quark degrees of freedom are neglected but mesonic excitations are included (see, for instance, Ref. [7]). We believe that our approach is more justified at high T and μ when constituent quarks become light but mesonic excitations are heavy (see below). Of course, due to the confining forces, at low T and μ quarks and antiquarks will recombine into mesons, baryons, and antibaryons. We can only hope that this hadronization process will not drastically change the character of the chiral transition that we study here. Then, up to an overall normalization factor,

$$\mathcal{Z}=\exp\left(-\frac{VU}{T}\right)\int\mathcal{D}\bar{q}\mathcal{D}q\exp\left\{\int_x\bar{q}[i\gamma^\mu\partial_\mu-g(\sigma+i\gamma_5\vec{\tau}\cdot\vec{\pi})]q+\mu\bar{q}\gamma^0 q\right\}=\exp\left(-\frac{VU}{T}\right)\det{}_p\{[p_\mu\gamma^\mu+\mu\gamma^0-g(\sigma+i\gamma_5\vec{\tau}\cdot\vec{\pi})]/T\}. \tag{4}$$

All thermodynamic quantities can now be obtained from the grand canonical potential

$$\Omega(T,\mu)=-\frac{T\ln\mathcal{Z}}{V}=U(\sigma,\vec{\pi})+\Omega_{q\bar{q}}, \tag{5}$$

where the contribution of quarks and antiquarks follows from Eq. (4):

$$\Omega_{q\bar{q}}(T,\mu)=-\nu_q\int\frac{d^3\mathbf{p}}{(2\pi)^3}\left\{E+T\ln\left[1+\exp\left(\frac{\mu-E}{T}\right)\right]+T\ln\left[1+\exp\left(\frac{-\mu-E}{T}\right)\right]\right\}. \tag{6}$$

Here, $\nu_q=2N_cN_f=12$ is the number of internal degrees of freedom of the quarks, $N_c=3$, and $E=\sqrt{p^2+M^2}$ is the valence quark and antiquark energy. The constituent quark (antiquark) mass M is defined to be

$$M^2=g^2(\sigma^2+\vec{\pi}^2). \tag{7}$$

The divergent first term in Eq. (6) comes from the negative energy states of the Dirac sea. As follows from the standard renormalization procedure it can be partly absorbed in the coupling constant λ^2 and the constant v^2. However, a logarithmic correction from the renormalization scale remains. This term is neglected in the following calculations. Similar logarithmic terms are explicitly included in calculations within the NJL model (see below). Therefore one can use the comparison of these two models to draw conclusions about the importance of these corrections.

After integrating Eq. (6) by parts the contribution of valence quarks and antiquarks can be rewritten as

$$\Omega_{q\bar{q}}(T,\mu)=-\frac{\nu_q}{6\pi^2}\int_0^\infty dp\frac{p^4}{E}[n_q(T,\mu)+n_{\bar{q}}(T,\mu)], \tag{8}$$

where n_q and $n_{\bar{q}}$ are the quark and antiquark occupation numbers,

$$n_q(T,\mu)=\frac{1}{1+\exp[(E-\mu)/T]},\quad n_{\bar{q}}(T,\mu)=n_q(T,-\mu). \tag{9}$$

The baryon chemical potential is determined by the net baryon density

$$n_B=-\frac{1}{3}\frac{\partial\Omega}{\partial\mu}=\frac{\nu_q}{6\pi^2}\int p^2dp[n_q(T,\mu)-n_{\bar{q}}(T,\mu)]. \tag{10}$$

The net quark density is obviously $n=3n_B$. The values for the σ and $\vec{\pi}$ fields and thereby the quark masses in Eq. (7) are obtained by minimizing Ω with respect to σ and $\vec{\pi}$,

$$\frac{\partial\Omega}{\partial\sigma}=\lambda^2(\sigma^2+\vec{\pi}^2-v^2)\sigma-H+g\rho_s=0, \tag{11}$$

$$\frac{\partial\Omega}{\partial\vec{\pi}}=\lambda^2(\sigma^2+\vec{\pi}^2-v^2)\vec{\pi}+g\vec{\rho}_{ps}=0. \tag{12}$$

The scalar and pseudoscalar densities of valence quarks and antiquarks can be expressed as [15]

$$\rho_s=\langle\bar{q}q\rangle=g\sigma\nu_q\int\frac{d^3\mathbf{p}}{(2\pi)^3}\frac{1}{E}[n_q(T,\mu)+n_{\bar{q}}(T,\mu)], \tag{13}$$

$$\vec{\rho}_{ps}=\langle\bar{q}i\gamma_5\vec{\tau}q\rangle=g\vec{\pi}\nu_q\int\frac{d^3\mathbf{p}}{(2\pi)^3}\frac{1}{E}[n_q(T,\mu)+n_{\bar{q}}(T,\mu)]. \tag{14}$$

These densities generate the source terms in the equations of motions for the meson fields (11) and (12). The minima of Ω defined by Eqs. (11) and (12) correspond to the stable or metastable states of matter in thermodynamical equilibrium where the pressure is $P=-\Omega_{min}$. The σ and pion masses are determined by the curvature of Ω at the global minimum:

$$M_\sigma^2=\frac{\partial^2\Omega}{\partial\sigma^2},\quad M_{\pi_i}^2=\frac{\partial^2\Omega}{\partial\pi_i^2}. \tag{15}$$

Explicitly they are given by the expressions

$$M_\sigma^2=m_\pi^2+\lambda^2\left(3\frac{M^2}{g^2}-f_\pi^2\right)+g^2\frac{\nu_q}{2\pi^2}\int dpp^2\left[\frac{p^2}{E^3}\left(\frac{1}{1+\exp[(E+\mu)/T]}+\frac{1}{1+\exp[(E-\mu)/T]}\right)\right.$$
$$\left.-\frac{M^2}{TE^2}\left(\frac{1}{2(1+\cosh[(E+\mu)/T])}+\frac{1}{2(1+\cosh[(E-\mu)/T])}\right)\right], \tag{16}$$

$$M_\pi^2=m_\pi^2+\lambda^2\left(\frac{M^2}{g^2}-f_\pi^2\right)+g^2\frac{\nu_q}{2\pi^2}\int dpp^2\frac{1}{E}\left[\frac{1}{1+\exp[(E+\mu)/T]}+\frac{1}{1+\exp[(E-\mu)/T]}\right]. \tag{17}$$

Here we have set the expectation value of the pion field to zero, $\vec{\pi}=0$, and thus $M^2=g^2\sigma^2$. This version of the sigma model was used earlier in Ref. [16] for thermodynamical calculations at nonzero T and $\mu=0$, and at nonzero μ and $T=0$. Some useful formulas for the case of a small quark mass are given in the Appendix.

III. THERMODYNAMICS OF THE NJL MODEL

The NJL model has been widely used earlier for describing hadron properties and the chiral phase transition [17,18]. The simplest version of the model including only scalar and pseudoscalar four-fermion interaction terms is given by the Lagrangian[1]

$$\mathcal{L}=\bar{q}(i\gamma^\mu\partial_\mu-m_0)q+\frac{G}{2}[(\bar{q}q)^2+(\bar{q}i\gamma_5\vec{\tau}q)^2], \tag{18}$$

where m_0 is the small current quark mass. At vanishing m_0 this NJL Lagrangian is invariant under chiral $SU(2)_L\times SU(2)_R$ transformations. Since the coupling constant G has dimension (energy)$^{-2}$, the theory is nonrenormalizable. Therefore, a three-momentum cutoff Λ is introduced to regularize divergent integrals. It defines an upper energy limit for this effective theory. With m_0 fixed at 5.5 MeV, free parameters of the model are chosen to reproduce correctly the

[1]As demonstrated in Ref. [19], the inclusion of the vector–axial vector terms may significantly change the parameters of the chiral phase transition, in particular, the position of the critical point. But this does not change the qualitative conclusions of the present paper.

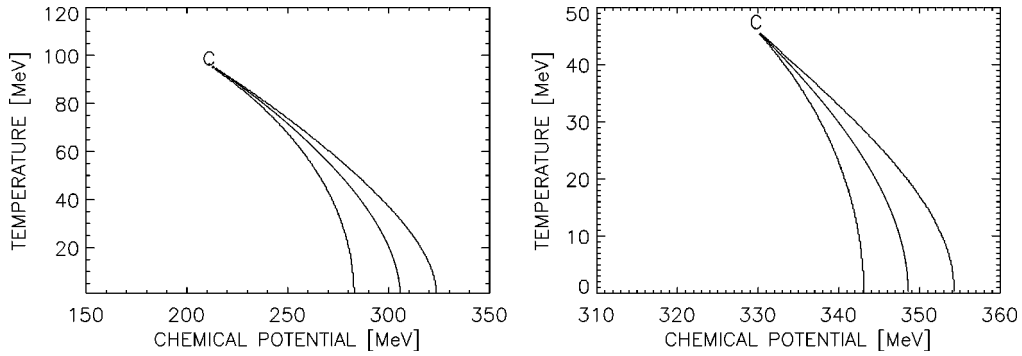

FIG. 1. The phase diagrams for the sigma model (left) and the NJL model (right) in the (μ,T) plane. The middle curve is the critical line and the outer lines are the lower and upper spinodal lines. C is the critical point.

vacuum values of the pion decay constant (93 MeV) and the pion mass (138 MeV). This gives the following parameters [20]: $G=5.496\ \mathrm{GeV}^{-2}$ and $\Lambda=631$ MeV. The constituent quark mass in vacuum is then 337 MeV. With these parameters the chiral transition occurs at the temperature $T\approx 190$ MeV [18] (for $\mu=0$), which is significantly higher than in the sigma model.

The partition function for the NJL model reads

$$\mathcal{Z}=\mathrm{Tr}\exp[-(\hat{\mathcal{H}}-\mu\hat{\mathcal{N}})]=\int \mathcal{D}\bar{q}\mathcal{D}q\exp\left[\int_x(\mathcal{L}+\mu\bar{q}\gamma^0 q)\right]. \tag{19}$$

In the mean-field approximation the Lagrangian (18) is represented in a linearized form [17,18,21]:

$$\mathcal{L}=\bar{q}(i\gamma^\mu\partial_\mu-m_0)q+G\langle\bar{q}q\rangle(\bar{q}q)-\frac{G}{2}\langle\bar{q}q\rangle^2, \tag{20}$$

such that the partition function becomes

$$\mathcal{Z}=\exp\left[-\frac{V}{T}\frac{G\langle\bar{q}q\rangle^2}{2}\right]\det{}_p[(p_\mu\gamma^\mu+\mu\gamma^0-M)/T], \tag{21}$$

where the constituent quark mass is determined from the gap equation

$$M=m_0-G\langle\bar{q}q\rangle. \tag{22}$$

The right-hand side of this equation involves the scalar density (chiral condensate)

$$\rho_s=\langle\bar{q}q\rangle=M\nu_q\int_{p<\Lambda}\frac{d^3\mathbf{p}}{(2\pi)^3}\frac{1}{E}[n_q(T,\mu)+n_{\bar{q}}(T,\mu)-1], \tag{23}$$

where n_q and $n_{\bar{q}}$ are the valence quark and antiquark occupation numbers defined in Eq. (9). Here the last term in brackets gives the contribution from the Dirac sea (which corresponds to the vacuum part of the sigma model) and cannot be neglected. The rest comes from valence quarks and antiquarks, similar to the sigma model [compare with Eq. (13)].

From Eq. (20), the grand canonical potential for the NJL model can be written as

$$\Omega=\frac{(M-m_0)^2}{2G}-\nu_q\int_{p<\Lambda}\frac{d^3\mathbf{p}}{(2\pi)^3}\left\{E+T\ln\left[1+\exp\left(-\frac{E+\mu}{T}\right)\right]+T\ln\left[1+\exp\left(-\frac{E-\mu}{T}\right)\right]\right\}. \tag{24}$$

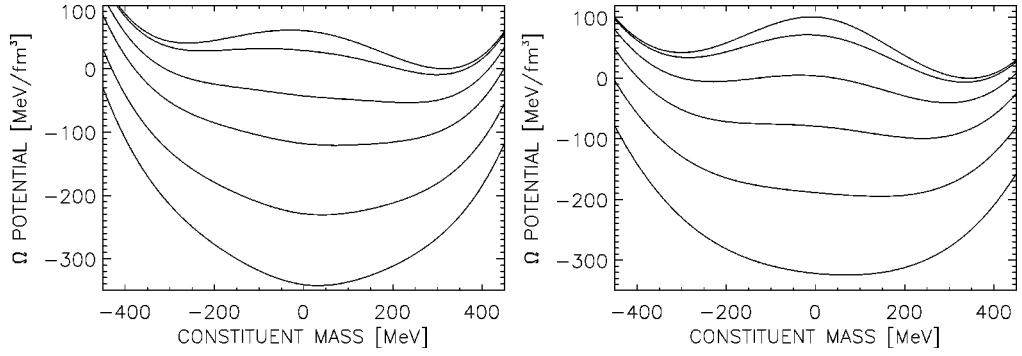

FIG. 2. The thermodynamical potentials Ω for the sigma model (left) and the NJL model (right). For both models $\mu=0$. The levels correspond to (starting from the top) $T=[0,100,135,155,175,190]$ MeV for the sigma model and $T=[0,100,140,170,200,230]$ MeV for the NJL model.

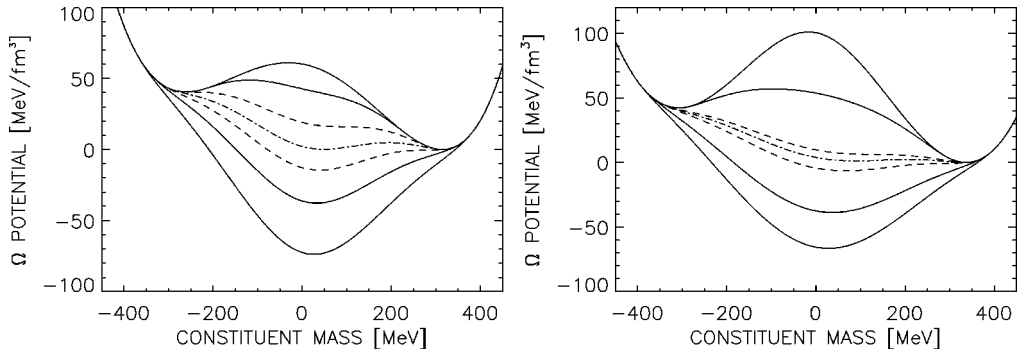

FIG. 3. The thermodynamical potentials Ω for the sigma model (left) and the NJL model (right). For both models $T=0$. The levels correspond to (starting from the top) $\mu=[0,225,279,306,322,345,375]$ MeV in the sigma model and $\mu=[0,288,343,348,35,378,396]$ MeV for the NJL model.

The minimization of Ω with respect to M gives the gap equation (22). The expression (24) is formally identical with Eq. (6) derived for the sigma model, but now the first term in curly brackets, coming from the Dirac sea, is treated explicitly after introducing the cutoff momentum Λ. One can calculate this vacuum contribution explicitly,

$$\Omega_{\rm vac}=-\nu_q\int_{p<\Lambda}\frac{d^3\mathbf{p}}{(2\pi)^3}\sqrt{p^2+M^2}$$
$$=-\frac{\nu_q\Lambda^4}{8\pi^2}\left[\sqrt{1+z^2}\left(1+\frac{z^2}{2}\right)-\frac{z^4}{2}\ln\frac{\sqrt{1+z^2}+1}{z}\right], \tag{25}$$

where $z=M/\Lambda$. Expanding this expression in powers of z one can obtain contributions to Ω of order M^2, M^4, ... As mentioned above, in the sigma model the vacuum terms are partly absorbed in the coefficients of the effective potential $U(\sigma,\vec{\pi})$. However, the logarithmic term $M^4\ln(\Lambda/M)$ cannot be removed in this way. Therefore, the NJL model has additional nonlinear terms in the vacuum energy which are responsible for the differences in the thermodynamic properties of the two models.

The sigma and pion masses are not as straightforward to obtain as in the linear sigma model because in the NJL model they are not represented as dynamical fields. In this model mesons are described as collective $q\bar{q}$ excitations. Their masses can be obtained from the poles of the quark-antiquark scattering amplitude which can be computed, for instance, in the random phase approximation (RPA) [18,20]. In this way, one can derive the following equations for the sigma and pion masses:

$$0=\frac{m_0}{M}+(M_\sigma^2-4M^2)GI(M,M_\sigma), \tag{26}$$

$$0=\frac{m_0}{M}+M_\pi^2 GI(M,M_\pi). \tag{27}$$

The function $I(x,y)$ is the quark-antiquark propagator defined as

$$I(x,y)=\frac{\nu_q}{2\pi^2}\mathcal{P}\int_{p<\Lambda}dpp^2\frac{1}{E}[1-n_q-n_{\bar{q}}]\frac{1}{E^2-1/4\,y^2}, \tag{28}$$

where $E=\sqrt{x^2+p^2}$, and the occupation numbers n_q and $n_{\bar{q}}$ are as defined in Eq. (9). In this integral $\mathcal{P}$ means principal value.

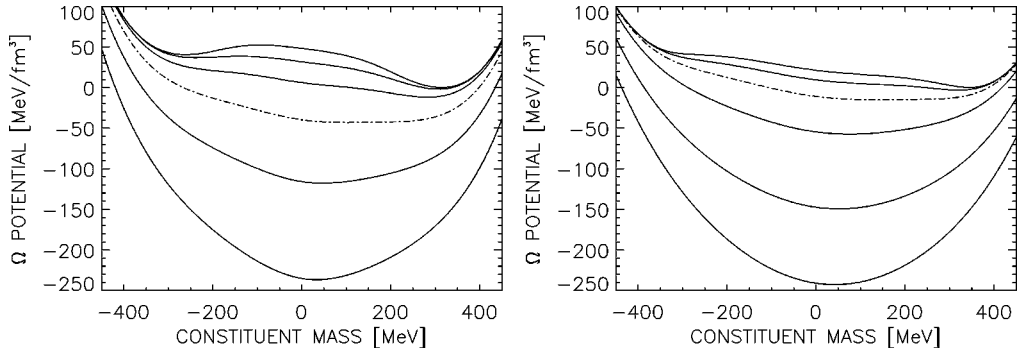

FIG. 4. The thermodynamical potentials Ω for the sigma model (left) and the NJL model (right). For the sigma model case μ is fixed to 207 MeV and the levels correspond to (starting from the top) $T=[0,50,75,100,125,150]$ MeV. For the NJL model case μ is fixed to 332 MeV and the levels correspond to (starting from the top) $T=[0,28,46,70,105,133]$ MeV.

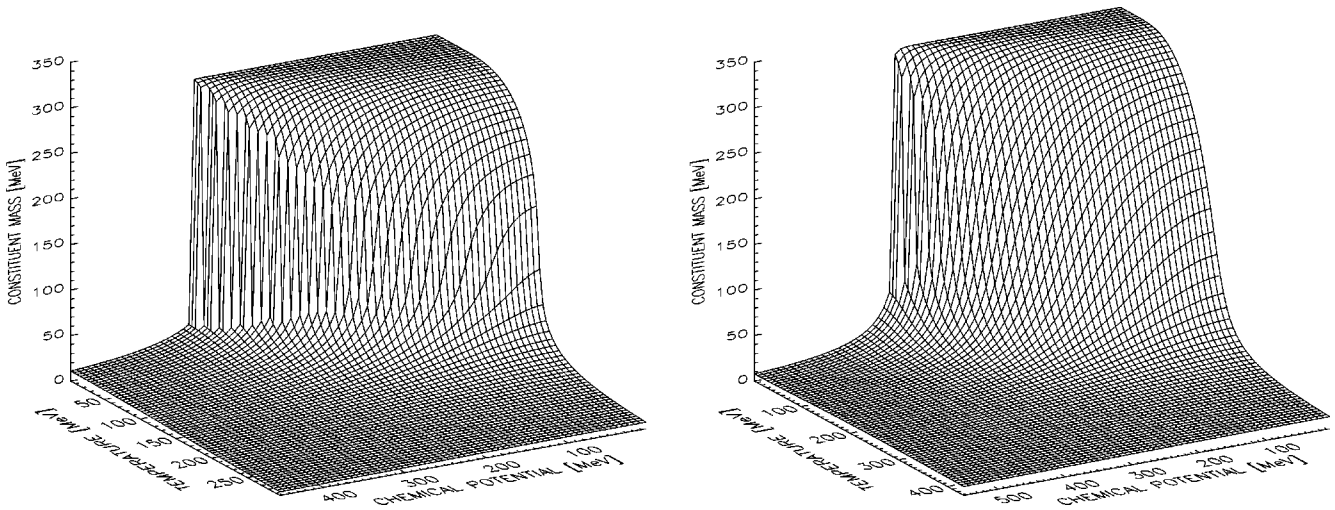

FIG. 5. The constituent quark (antiquark) mass in the sigma model (left) and the NJL model (right) as a function of μ and T.

IV. NUMERICAL RESULTS

In the case of the linear sigma model everything is determined when the gap equation (11) is solved in the (T,μ) plane, whereas in the NJL model the meson masses have to be solved for as well. Below we present results of our numerical calculations (see also the Appendix).

A. Phase diagrams

As our calculations show, both models exhibit a first order chiral phase transition at $T<T_c$ and nonzero chemical potential. In Fig. 1 we present the resulting phase diagrams in the (T,μ) plane calculated for the two models. The middle line corresponds to the states where two phases coexist in the first order phase transition. Along this line the thermodynamic potential Ω has two minima of equal depth separated by a potential barrier whose height grows toward lower temperatures. At the critical point C the barrier disappears and the transition is of second order. The other lines in Fig. 1 are spinodal lines which constrain the regions of spinodal instability where $(\partial n_B/\partial\mu)_T<0$. Information about the time scales of this instability is important for dynamical simulations [4,5,16,23,24].

It is instructive to plot the thermodynamic potential as a function of the order parameter for various values of T at $\mu=0$, and for various values of μ at $T=0$. The first case is shown in Fig. 2, where the left panel is for the sigma model and the right panel for the NJL model. One clearly sees the smooth crossover of the symmetry breaking pattern in both cases. Note that the effective bag constant (the energy difference between the global minimum and the local maximum of the potential in vacuum) is about 100 MeV/fm^3 in the NJL model, whereas in the sigma model it is significantly smaller, $\simeq 60$ MeV/fm^3. To a large extent this difference is responsible for the difference in the temperatures corresponding to the crossover transition: about 140 MeV in the sigma model and about 180–190 MeV in the NJL model.

In Fig. 3 the same plot is shown for $T=0$ and a nonzero μ. Here, one clearly observes the pattern characteristic of a first order phase transition: two minima corresponding to phases of restored and broken symmetry separated by a potential barrier. The barrier height is larger in the sigma model than in the NJL model, thus indicating a weaker first order phase transition in the NJL model. It now follows that somewhere in between these two extremes, for some μ_c and T_c, there exists a critical point for a second order phase transition. Indeed, this point is found and shown in Fig. 1. The corresponding values are $(T_c,\mu_c)\simeq(99,207)$ MeV in the sigma model, and $(T_c,\mu_c)\simeq(46,332)$ MeV in the NJL model. The behavior of the thermodynamic potential at μ

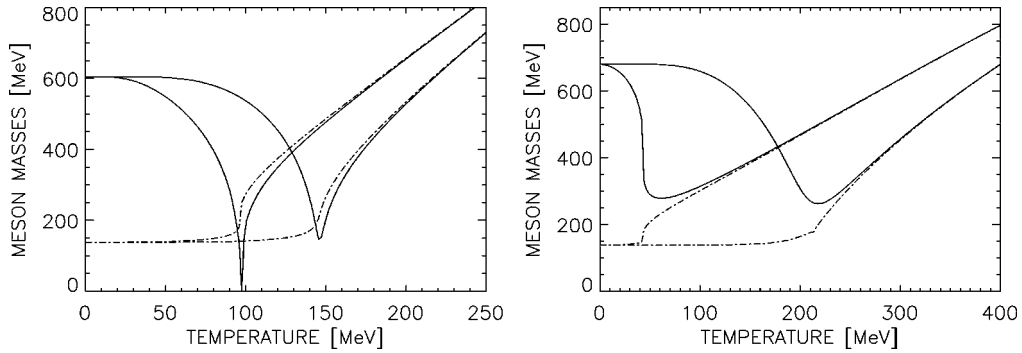

FIG. 6. The sigma mass (solid line) and pion mass (dashed line) in the sigma model (left) and NJL model (right) as functions of temperature for $\mu=0$ (right pair) and for $\mu=\mu_c$ (left pair).

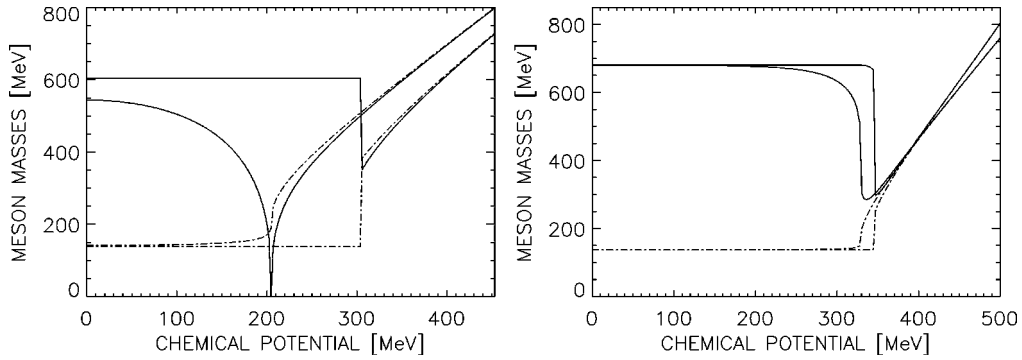

FIG. 7. The sigma mass (solid line) and pion mass (dashed line) in the sigma model (left) and NJL model (right) as functions of chemical potential for $T=0$ (right pair) and for $T=T_c$ (left pair).

$=\mu_c$ and various T is shown in Fig. 4. One can see that the potential has only one minimum which is flattest at the critical point.

B. Effective masses

Now let us consider the model predictions for the effective masses. The constituent quark mass is shown in Fig. 5 as a function of T and μ. These plots, of course, show the same phase structure as discussed above. At $\mu=0$ in both models the quark mass falls smoothly from the corresponding vacuum value and approaches zero as T goes to infinity. One could define a crossover temperature as corresponding to a steepest descent region in the variation of M. This again gives a temperature of about 140–150 MeV for the sigma model and about 180–190 MeV for the NJL model. At $T=0$ and nonzero μ the constituent quark mass shows a discontinuous behavior reflecting a first order chiral transition.

The sigma and pion masses for various T and μ are shown in Figs. 6 and 7. In both models the sigma mass first decreases smoothly and then rebounds and grows again at high T. The pion mass does not change much at temperatures below T_c but then increases rapidly, approaching the sigma mass and signaling the restoration of chiral symmetry. At large T the masses grow linearly with increasing T (see the Appendix). The $\mu=\mu_c$ case is especially interesting in the sigma model. Since the sigma field is the order parameter of the chiral phase transition, its mass must vanish at the critical point for a second order phase transition. This means that Ω has zero curvature at this point. It is, however, not clear what the sigma mass should be at the critical point in the NJL model where the quark condensate $\langle\bar{q}q\rangle$ is the order parameter. Figure 6 indeed shows that the sigma mass is zero exactly at the critical point in the sigma model. This is not the case in the NJL model, at least within the RPA used here.

In Fig. 7 the masses are plotted as a function of μ for $T=0$ and $T=T_c$. For $T=0$ one clearly sees discontinuities in the behavior of the masses, characteristic of a first order phase transition.

An interesting point is that, in the linear sigma model, there is no stable phase with heavy quarks for $T=0$, i.e., the quark mass assumes its vacuum value all the way up to the chiral transition, and then drops to a small value in the phase where chiral symmetry is restored (see Fig. 7). This behavior is related to the appearance of a bound state at zero pressure. Within the linear sigma model this ''abnormal'' bound state was found by Lee and Wick a long time ago [22]. Recently, it was shown in Ref. [19] that a similar bound state appears also in the NJL model. This behavior, however, depends on the values of the coupling constants g or G. For our choice of g and G, this behavior is more pronounced in the linear sigma model (see Fig. 5). In general, if the coupling constant is sufficiently large, the attractive force between the constituent quarks becomes large enough to counterbalance the Fermi pressure, thus giving rise to a bound state. To demon-

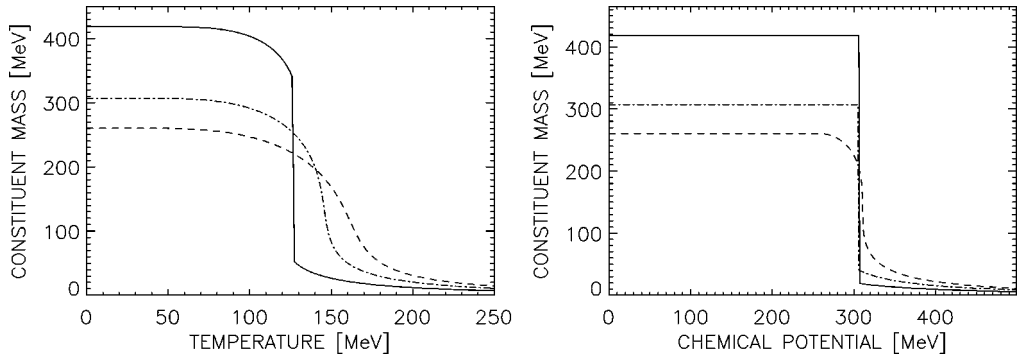

FIG. 8. The constituent quark (antiquark) mass as a function of temperature for zero chemical potential (left) and as a function of chemical potential for zero temperature (right) in the sigma model. The solid line represents the mass for $g=4.5$, the dash-dotted line for $g=3.3$, and the dashed line for $g=2.8$.

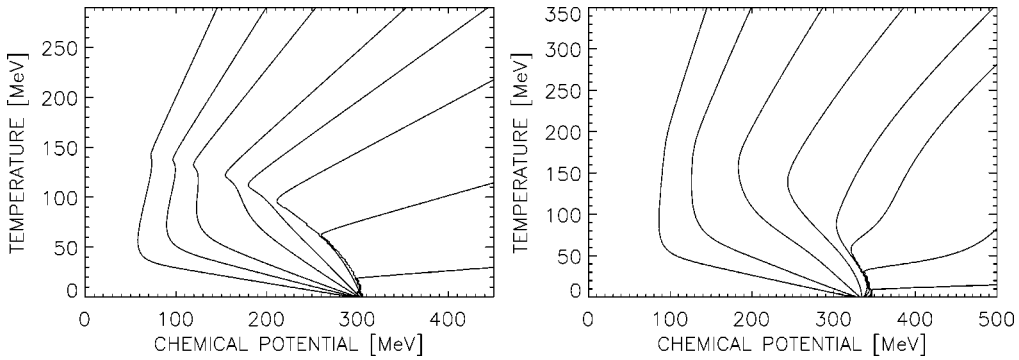

FIG. 9. The entropy per baryon number S/A for the sigma model (left) and the NJL model (right). In the sigma model the curves correspond to (from left) $S/A=[28,21,17,13,11,9,6,2]$. In the NJL model the curves correspond to (from left) $S/A=[22,16,11,8,6,5,3,1]$.

strate this we have varied the coupling constant g for the sigma model within reasonable limits.

The results for the quark mass are shown in Fig. 8. It is seen that, indeed, one can change the smooth crossover for $\mu=0$ into a first order transition by increasing the coupling constant (Fig. 8 left panel) and change the first order transition in the case of $T=0$ into a smooth crossover. In this way a heavy quark phase comes into existence as the coupling constant is decreased and the bound state disappears (Fig. 8 right panel). An analogous investigation for the NJL model leads to similar results.

C. Adiabats

Regarding hydrodynamical simulations the entropy per baryon S/A is an interesting quantity. One can easily calculate it using standard thermodynamic relations,

$$\frac{S}{A}=3\frac{e+p-\mu n}{Tn}, \tag{29}$$

where e, p, and n are, respectively, the energy density, pressure, and net density of quarks and antiquarks ($n=3n_B$). By studying this quantity, one can check if there is a tendency toward convergence of the adiabats toward the critical point as was claimed in Ref. [6]. If this was the case it would be easy to actually hit or go close to this point in a hydrodynamical evolution. Figure 9 shows the contours of S/A in the (T,μ) plane calculated in the sigma model (left) and in the NJL model (right). We actually observe a trend that is quite opposite to this expectation. It turns out that the adiabats turn away from the critical point when they hit the first order transition line and bend toward the critical point only when they come from the smooth crossover region. This is explained as follows. First, note that all adiabats terminate at zero temperature and $\mu=M_{\rm vac}$, i.e., the (T,μ) combination corresponding to the vacuum. The reason is that as $T\to 0$ also $S\to 0$ (by the third law of thermodynamics); therefore, for fixed S/A we have to require that $n\to 0$, which is fulfilled when $\mu=M_{\rm vac}$. For our choice of parameters, in the sigma model the point $(T,\mu)=(0,M_{\rm vac})$ is also the end point of the phase transition curve at $T=0$, since the phase transition connects the vacuum directly with the phase of restored chiral symmetry; cf. Figs. 5 and 8. For the NJL model, the end point of the phase transition curve is not identical with $(0,M_{\rm vac})$ but is rather close to it. Therefore, the adiabats that hit the phase transition curve also have to bend away from the critical point and approach the end point of the phase transition line at $T=0$, i.e., T decreases and μ increases.

This behavior is quite opposite to the case underlying the claim in Ref. [6], where the hadronization of a large number of quark and gluon degrees of freedom into relatively few pion degrees of freedom leads to the release of latent heat and consequently to a reheating (increase of T) through the phase transition. Remember, however, that in our case there is actually no change in the number of degrees of freedom in the two phases. The change is only in the respective quark masses. Consequently, there is no ''focusing'' effect in the linear sigma and NJL models.

On the other hand, the behavior of the adiabats in Fig. 9 is quite typical for an ordinary liquid-gas phase transition. Here liquid and gas are represented, respectively, by chirally symmetric and broken phases. This analogy was further elaborated in Ref. [19].

V. CONCLUSIONS

We investigated the thermodynamics of the chiral phase transition within the linear sigma model coupled to quarks and the Nambu–Jona-Lasinio model. These models have similar vacuum properties but treat the contribution of the Dirac sea differently. In the sigma model this contribution is ''renormalized out'' while in the NJL model it is included explicitly up to a momentum cutoff Λ. By comparing thermodynamic properties of these two models one can check the importance of these vacuum terms. In both models, for small bare quark masses, we have found a smooth crossover for nonzero temperature and zero chemical potential and a first order transition for zero temperature and nonzero chemical potential. The first order phase transition line in the (T,μ) plane ends in the expected critical point. It has been found that the σ mass is zero at the critical point in the sigma model whereas in the NJL model it always remains nonzero. The behavior of the adiabats in both models shows a pattern opposite to the expectations for the chiral/confinement transition of [6]. In fact, the phase transition found in these two models turned out to be of the liquid-gas type. However, the strength of this phase transition depends significantly on the

coupling constants of the models. From the comparison we conclude that the phase transition pattern is generally weaker in the NJL model than in the sigma model. This is mainly due to additional vacuum terms discussed above. Certainly, it will be interesting to use both models in hydrodynamical simulations in order to confirm or disprove possible observable signatures of the phase transition discussed in the introduction. In particular, the sigma model, which contains dynamical σ and pion fields, would be suitable to study the long wavelength enhancement of the σ field at the critical point. Such simulations are in progress.

ACKNOWLEDGMENTS

The authors thank J. Borg, L. P. Csernai, P. Ellis, B. Friman, A. D. Jackson, L. M. Satarov, and A. Wynveen for useful discussions. O.S. thanks the Yale Relativistic Heavy Ion Group for kind hospitality and support from Grant No. DE-FG02-91ER-40609. The work of A.M. is supported by the U.S. Department of Energy under Grant No. DE-FG02-87ER40328. I.N.M. thanks the Humboldt Foundation for financial support. D.H.R. thanks RIKEN, BNL, and the U.S. Department of Energy for providing the facilities essential for the completion of this work.

APPENDIX

In the chirally symmetric phase the constituent quark (antiquark) mass M is small; it goes to zero in the chiral limit. Therefore, it is instructive to evaluate the thermodynamic potential $\Omega(T,\mu,M)$ for small M. In this limit $\Omega_{q\bar{q}}$ can be represented as a power series in M. Below we give explicit expressions for the sigma model. Taking into account that $\Omega_{q\bar{q}}$ is an even function of M, one can write

$$\Omega_{q\bar{q}}(T,\mu;M)=\Omega_0(T,\mu)+\frac{M^2}{2}\left(\frac{\partial^2\Omega_{q\bar{q}}}{\partial M^2}\right)_{M=0}+\cdots. \tag{A1}$$

Here the first term $\Omega_0(T,\mu)\equiv\Omega_{q\bar{q}}(T,\mu,0)$ can easily be calculated for arbitrary T and μ. The well-known result is

$$\Omega_0(T,\mu)=-\frac{\nu_q}{2\pi^2}\left[\frac{7\pi^4}{180}T^4+\frac{\pi^2}{6}T^2\mu^2+\frac{1}{12}\mu^4\right]. \tag{A2}$$

The quark number and entropy densities for massless fermions are obtained by differentiating $\Omega_0(T,\mu)$ with respect to μ and T, respectively,

$$n=\frac{\nu_q}{6\pi^2}(\pi^2T^2\mu+\mu^3), \tag{A3}$$

$$s=\frac{\nu_q}{6\pi^2}\left(\frac{7\pi^4}{15}T^3+\pi^2T\mu^2\right). \tag{A4}$$

The second term in Eq. (A1) differs only by a factor of M from the scalar density defined in Eq. (13). A straightforward calculation gives

$$\left(\frac{\partial^2\Omega}{\partial M^2}\right)_{M=0}=\left(\frac{\rho_s}{M}\right)_{M\to0}=\nu_q\left(\frac{T^2}{12}+\frac{\mu^2}{4\pi^2}\right). \tag{A5}$$

This can be used to estimate the pion and sigma masses at large T and/or μ. Expressing M^2 in terms of mean π and σ fields, Eq. (15), and using the definition of effective masses from Eq. (7), one arrives at the following asymptotic ($M\to0$) expression for the pion and sigma masses:

$$M_\pi^2=M_\sigma^2=g^2\nu_q\left(\frac{T^2}{12}+\frac{\mu^2}{4\pi^2}\right). \tag{A6}$$

It shows that deep in the chiral symmetric phase the pion and sigma masses are degenerate and large. At high temperatures ($T\gg\mu$), $M_\pi=M_\sigma=gT$, where $g\sim3$ in our calculations. Therefore, the contribution of pion and sigma excitations to the thermodynamical potential is suppressed by the Boltzmann factor $e^{-M_\sigma/T}=e^{-g}$.

In the case of the NJL model the above expressions are slightly modified due to the finite cutoff Λ in the momentum integration.

[1] See, for instance, F. Karsch, hep-lat/9909006.
[2] D. H. Rischke and M. Gyulassy, Nucl. Phys. **A608**, 479 (1996).
[3] I. N. Mishustin, Phys. Rev. Lett. **82**, 4779 (1999).
[4] I. N. Mishustin and O. Scavenius, Phys. Rev. Lett. **83**, 3134 (1999).
[5] O. Scavenius and A. Dumitru, Phys. Rev. Lett. **83**, 4697 (1999).
[6] M. Stephanov, K. Rajagopal, and E. Shuryak, Phys. Rev. Lett. **81**, 4816 (1998).
[7] J. Randrup, Phys. Rev. D **55**, 1188 (1997).
[8] M. A. Halasz, A. D. Jackson, R. E. Shrock, M. A. Stephanov, and J. J. Verbaarschot, Phys. Rev. D **58**, 096007 (1998).
[9] T. M. Schwarz, S. P. Klevansky, and G. Papp, Phys. Rev. C **60**, 055205 (1999).
[10] M. Alford, K. Rajagopal, and F. Wilczek, Phys. Lett. B **422**, 247 (1998).
[11] R. D. Pisarski and F. Wilczek, Phys. Rev. D **29**, 338 (1984).
[12] S. D. Hsu and M. Schwetz, Phys. Lett. B **432**, 203 (1998).
[13] M. Gell-Mann and M. Levy, Nuovo Cimento **16**, 705 (1960).
[14] Y. Nambu and G. Jona-Lasinio, Phys. Rev. **122**, 345 (1961).
[15] L. P. Csernai and I. N. Mishustin, Phys. Rev. Lett. **74**, 5005 (1995).
[16] L. P. Csernai, A. Mocsy, and I. N. Mishustin, Heavy Ion Phys. **3**, 151 (1996).
[17] U. Vogl and W. Weise, Prog. Part. Nucl. Phys. **27**, 195 (1991).
[18] S. P. Klevansky, Rev. Mod. Phys. **64**, 649 (1992).
[19] I. N. Mishustin, L. M. Satarov, H. Stöcker, and W. Greiner, Phys. Rev. C **62**, 034901 (2000).
[20] M. Asakawa and K. Yazaki, Nucl. Phys. **A504**, 668 (1989).

[21] D. H. Rischke and W. Greiner, Int. J. Mod. Phys. E **3**, 1157 (1994).
[22] T. D. Lee and G. C. Wick, Phys. Rev. D **9**, 2291 (1974).
[23] O. Scavenius, A. Dumitru, E. S. Fraga, J. T. Lenaghan, and A. D. Jackson, Phys. Rev. D (to be published), hep-ph/0009171.
[24] W. H. Press, S. A. Teukolsky, W. T. Vetterling, and B. P. Flannery, *Numerical Recipes in C*, 2nd ed. (Cambridge University Press, Cambridge, 1992).